25th ABCM International Congress of Mechanical Engineering
October 20-25, 2019, Uberlândia, MG, Brazil

COB-2019-1026
EVOLUTION OF MICROSTRUCTURE AND MECHANICAL PROPERTIES DURING THE COLD ROLLING OF AN AL0.4WT% W ALLOY SOLIDIFIED UNIDIRECTIONALLY

Sarah Maria de Albuquerque Sousa
Thiago Primo Sousa
Maycol Moreira Coutinho
Daniel Monteiro Rosa
Universidade de Brasília, Asa Norte – Brasília/ DF, 70910-900
albuquerque.sm4@gmail.com, tprimosousa@gmail.com, maycol.coutinho@gmail.com, danielrosa@unb.br

Abstract. *Aluminum alloys are receiving more attention and study interest due to their versatility and application in the most varied sectors. This work seeks to investigate the correlation between microstructure and mechanical properties of cold rolled Al0.4wt% W alloy. For this purpose, an Al0.4wt% W alloy was solidified unidirectionally, the thermal variables of the process were measured and samples were taken from different heights of the ingot to produce wires by cold rolling. To compare the samples between the lamination passes a qualitative analysis of the metallographic and a hardness assay were made. The macrostructure showed a predominantly columnar zone, the microstructure was more refined for higher cooling rates and the hardness increased as the deformation increased. Cold work proved to be an efficient mechanism of hardness increase, promoting even 62% hardness increase for area reduction of 79%. The specimen with higher tungsten concentration showed higher sensitivity to cold work showing greater percentage hardness increase, inferring that the addition of tungsten influences the disagreement movement.*

Keywords: *Microstructure, unidirectional solidification, cold rolling*

1. INTRODUCTION

The behavior of metallic products can be understood and predicted through the microstructure present in the metal, so the understanding of phenomena such as solidification and conformation are fundamental to control the microstructure thus enabling the optimization of the properties of the final product. In this context, aluminum is of great interest due to its versatility because its applications serve the most diverse industrial sectors such as automotive, transportation, electrical among others. Although the application of pure aluminum already has advantages over other materials, alloy elements are added to the matrix to modify mechanical properties such as hardness, tensile strength and yield strength (ASM Handbook Vol. 2, 1992). Sometimes impurity in the matrix behaves as a nucleating agent producing finer grains in the matrix and consequently making it difficult to move disagreements (Reed-Hill, 1982).

Solidification is one of the most usual ways of manufacturing metal alloys, where once the composition of the alloy is defined it will be the dynamic of this process that will define the structure of the metal, not only of castings, but also of the products that will be shaped. The mechanical characteristics of this product depend on grain size, dendritic spacing, lamellar or fibrous spacings of chemical composition heterogeneities, size, shape and distribution of inclusions, porosity formed, among others, where all these characteristics result from the conditions imposed by the variables. present in the solidification process. (Garcia, 2007). In the experimental study of solidification phenomena, the unidirectional solidification technique has been widely used for the characterization of microstructure aspects and mechanical properties (Rosa, 2007; Freitas, 2011; Reyes et. Al., 2017; Rodrigues, 2018; Şahin et al., 2018).

Another interesting phenomenon of study is the mechanical conformation that is an operation that uses the plastic deformation of the metals to obtain geometries of interest, this process is an important part of the industrial sector since the metals usually solidified in simple geometries (ingots and billets) need to be shaped to suit practical applications such as pipes, bars, thin plates, wires, e.g.. In addition to changing dimensions, conformation commonly promotes microstructural changes in the molten material and consequently in its properties (Helman and Cetlin, 2012).

The microstructure of a metal undergoes successive changes during plastic deformation, initially there is change in the shape of the grains, which become more elongated due to the compression effort and also the total area of grain contours increases (Calçada, 2018; Oliveira, 2009). Cold deformation confers hardening, increases tensile and yield strength limits, a good surface finish and precise dimensional control (Helman and Cetlin, 2012; Chiaverini, 1986).

Thus, the addition of tungsten and the degree of refining achieved during solidification can be influence the conformability of aluminum and this influence deserves to be investigated, since the literature presents little information about this alloy.

2. EXPERIMENTAL PROCEDURES

The alloy was prepared with commercially pure aluminum and tungsten at 0.4 wt%. Initially the aluminum was placed inside an alumina-coated crucible and melted in a muffle furnace with a working temperature of 1200 ºC. Once the aluminum melted, the tungsten was added to the crucible where it remained in the oven for four days, being stirred at regular times to favor the diffusion process.

After melting and homogenization the liquid temperature (T_L) was measured and the alloy was poured into the liquid mold. For the experiment, the alloy was remelted into the experimental furnace, avoiding convection caused by the initial casting.

The solidification was performed in a device designed to unidirectionally ascend heat, which consists of two cameras; a refrigerator where water circulates cooling the alloy represented by (3) and another where liquid metal is poured represented by (5) according to Figure 1.

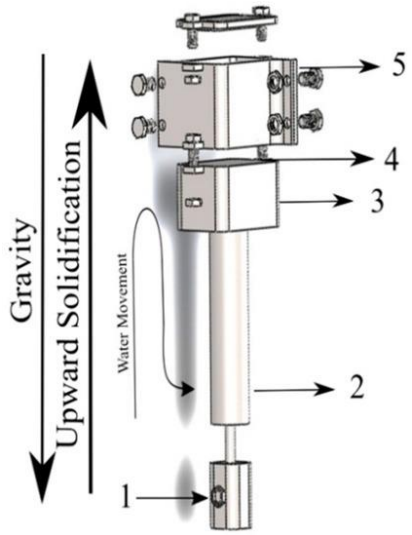

Figure 1. Experimental apparatus used in solidification. Source: Coutinho et al., 2019.

In the camera (5) were distributed seven type K thermocouples that allowed to define the thermal variables of the process at different heights. Cooling occurs by contacting the liquid metal with the bottom of the mold, represented by (4), which is constantly cooled by circulating water. In this system, as the solidified layer advances in front of the liquid, the thermal resistance increases, thus making it difficult to remove heat and reducing cooling speeds and rates to farther positions of the mold bottom in contact with water (Sousa, 2019; Coutinho et al., 2019)

The cooling system was triggered when the thermocouple temperature closest to the water flow reached 5% higher than the alloy T_L, ensuring that all metal was in liquid state. Thermal data acquired at the foundry were monitored during solidification at a frequency of 1 Hz.

The manufactured ingot was divided into four slices; one of the central slices was used to reveal the ingot macrostructure and perform chemical analysis of the sample and the other central slice was used to produce the specimens that were rolled. Specimens removed for lamination were identified as specimen one (CP1), specimen two (CP2) and specimen three (CP3). The height relative to the center plate/mold of each sample is equal to 6.55mm, 33.76mm and 47.86mm respectively. As the objective was to laminar using round profile the samples were machined in 7mm diameter cylinders. The illustrative scheme of the specimens is presented in Figure 2.

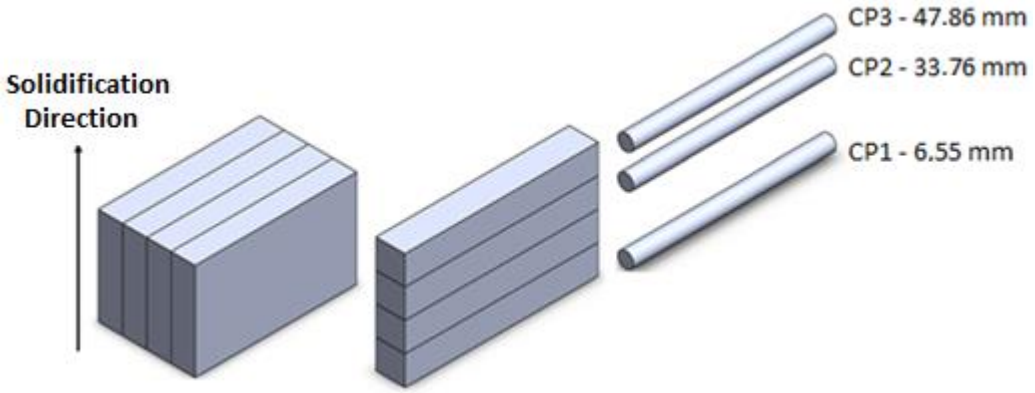

Figure 2. Illustrative scheme of separation of proof bodies.

Lamination was performed at room temperature using a Mascote Electric Laminator, shown in Figure 3.

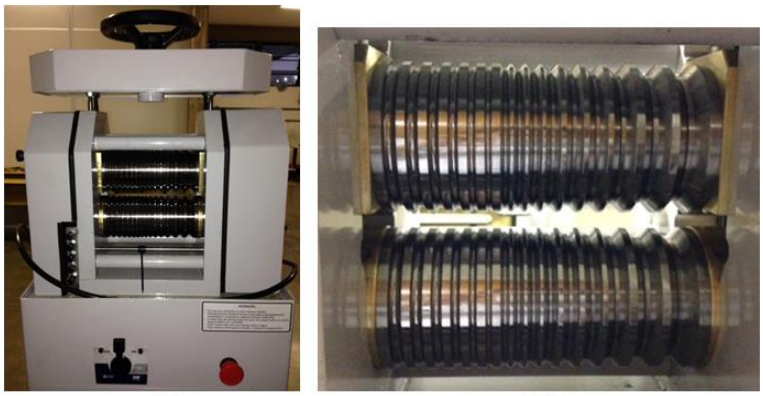

Figure 3. (a) Laminator (b) Laminator Roll Profile.

The samples were deformed in five lamination passes through the passage in each of the rolling section circular profiles. After each wire reduction, two samples were taken: one longitudinal and one transverse to the rolling direction. The thickness of each specimen was measured before and after lamination in order to calculate the deformation by reducing the area. As the objective of the study is to analyze the evolution of the metal from the molten state to the shaped state, samples of the material in the raw melt state were also analyzed.

To examine the macrostructures and microstructures, metallographic techniques were used according to ABNT NBR 13284. To reveal the macrostructure the surface closest to the center of the ingot was attacked with a Flick solution (10 mL HF, 15 mL HCL and 10 mL H_2O). For the microstructure the samples were chemically attacked with attack No. 12 (50ml Polton Reagent, 25ml HNO_3, 40ml solution of 3g chromic acid in 10ml H_2O), indicated by ASM Handbook Vol. 9 to reveal grain in aluminum alloys. Image processing was performed using the Olympus LEXT OLS 4000 confocal microscope

For the Vickers microhardness test, 10 random indentations were performed on each 50 gf loaded sample with an EmcoTest microdurometer DuraScan model 20 (Oliveira, 2009). The result was the mean of the measurements and the degree of dispersion in relation to the mean was calculated by the standard deviation function.

3. RESULTS AND DISCUSSIONS

3.1 Chemical Analysis

Table 1 quantitatively represents the chemical composition of the alloy at three different heights with respect to the die plate, these positions referring to the center of each specimen analyzed in the work. The results are related to the energy dispersion x-ray spectroscopy (EDX) and are in weight percentage of the three elements in greater quantity in the alloy.

Table 1. Chemical composition of the three specimens analyzed at work.

Position (mm)	Alloy Elements (% p)		
	Aluminum	Tungsten	Iron
47.86	99.040	0.175	0.347
33.76	98.764	0.257	0.382
6.55	98.970	0.182	0.463

3.2 Thermal Variables

The measured liquidus temperature (T_L) was 650.65° C, although lower than the tungsten melting temperature, the results of the EDX chemical tests revealed an alloy element distribution along the ingot indicating, that there was fusion through the process of diffusion of tungsten in the liquid aluminum bath, a similar process is performed for high melting elements such as Nb (Pisch, 2019).

By plotting the time at which the isotherm liquidus passes a given position against the corresponding thermocouple height, the isotherm liquidus velocity curve (V_L) was obtained as a function of position, as shown in Figure 4. The cooling rate ($\dot{T}$) was obtained by the ratio between the temperature and time intervals obtained before and after the passage of the liquidus isotherm for each thermocouple according to Figure 5.

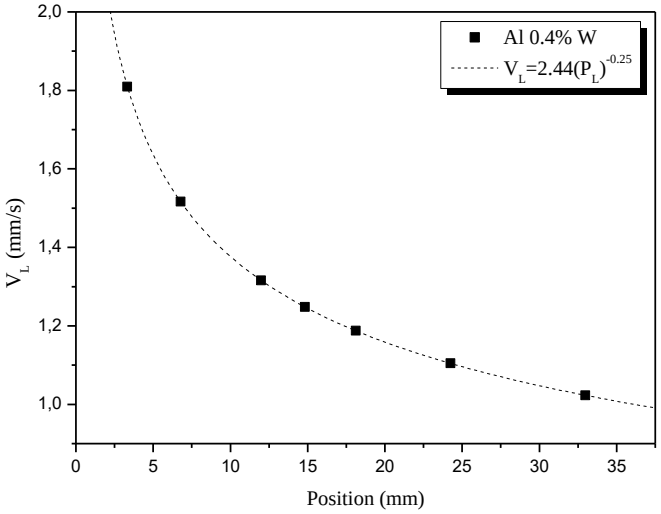

Figure 4. Speed of the liquidus isotherm.

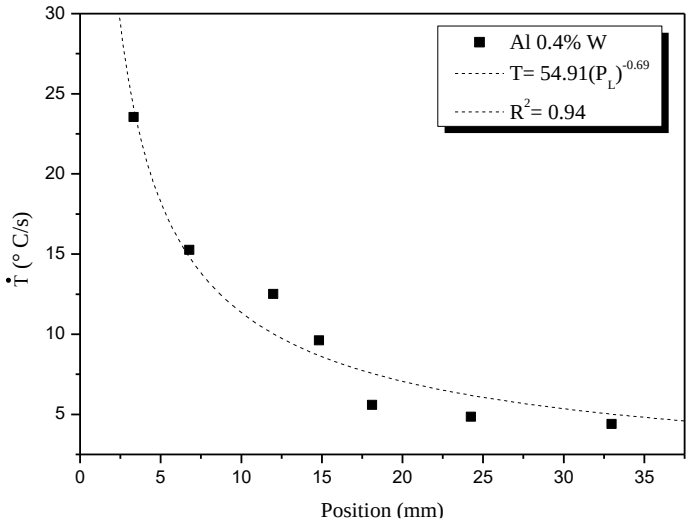

Figure 5. Cooling rate as a function of position from the metal/mold interface.

The curves of the thermal variables V_L and $\dot{T}$ (Figure 4 and Figure 5) show a decreasing profile from the moment they move away from the metal/mold interface. This occurs because the speed of solidification assumes relatively high

values at the beginning of the process and decreases gradually due to the thermal resistance of the growing solidified layer (Garcia, 2007).

3.3 Macrostructure

Figure 6 shows the solidification macrostructure of 0.4wt% W Al alloys. The macrostructure is composed of a predominantly columnar morphology. This directionality is due to the heat extraction flow and attests to unidirectional solidification.

Figure 6. Typical directionally solidified macrostructures for alloys Al–0.4wt W (wt.%).

3.4 Microstructure

The aluminum alloy was rolled in a total of five passes, obtaining an area reduction of approximately 79%, with a starting diameter of 7 mm and a final diameter of 3.2 mm. Figure 7, Figure 8 and Figure 9 show the microstructural characterization of the alloy in the raw melt state and after each reduction pass. The microstructure analysis was performed in the longitudinal section because the effects of deformation were more evident than in the cross section.

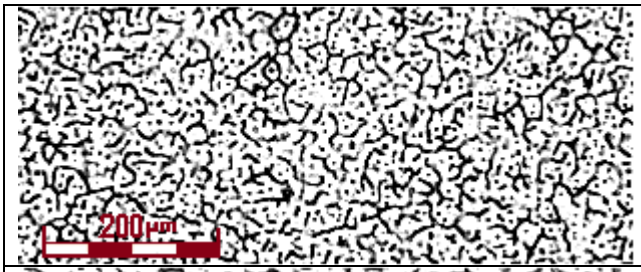	CP1 – 6.55 mm Molten state
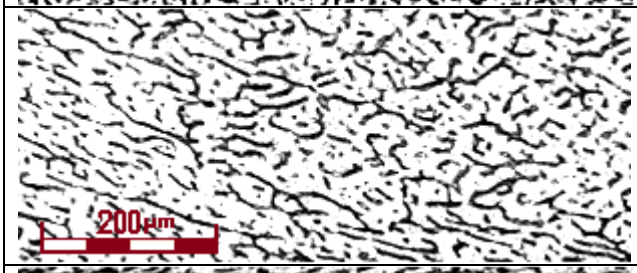	CP1 - 6.55 mm 50.57% of deformation
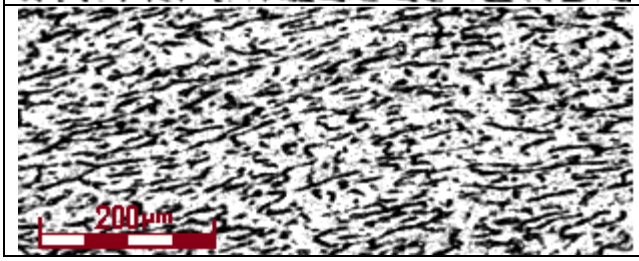	CP1 - 6.55 mm 78.67% of deformation

Figure 7. Specimen 1 microstructure, before and after deformation, 100X magnification.

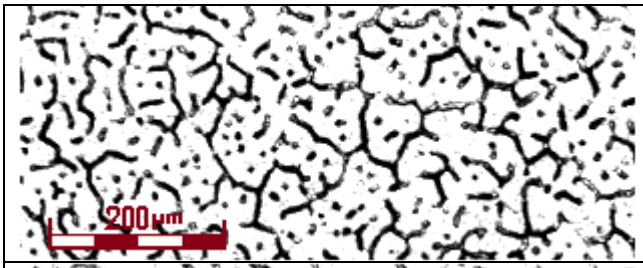	CP2 –33.76 mm Molten state
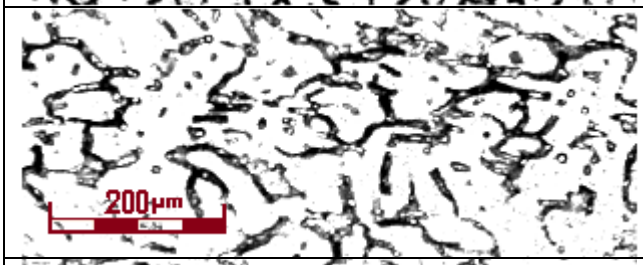	CP2 – 33.76 mm 50.57% of deformation
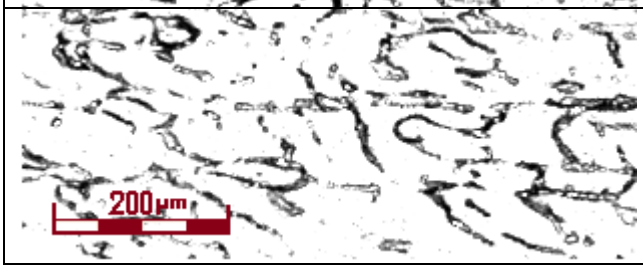	CP2 – 33.76 mm 78.67% of deformation

Figure 8. Specimen 2 microstructure, before and after deformation, 100X magnification.

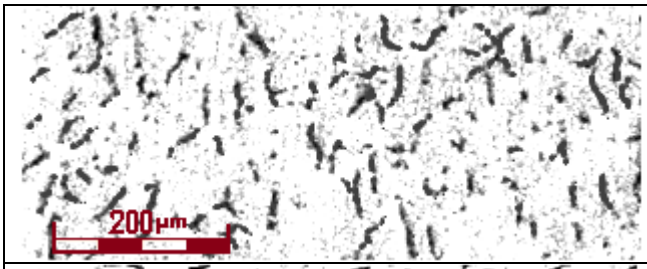	CP3 – 47.86 mm Molten state
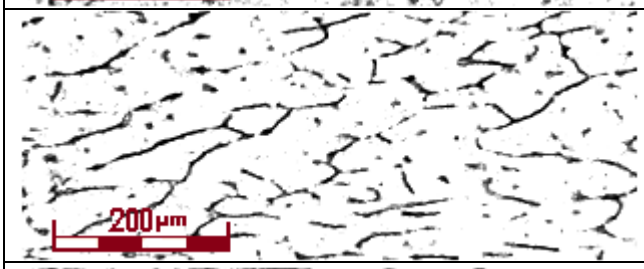	CP3 – 47.86 mm 50.57% of deformation
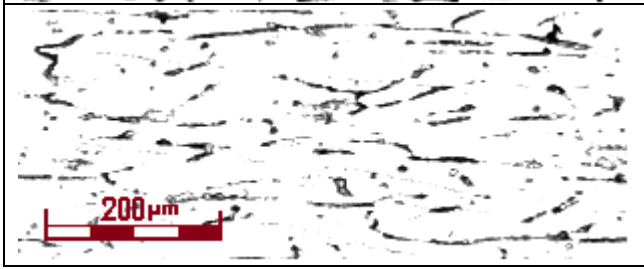	CP3 – 47.86 mm 78.67% of deformation

Figure 9. Specimen 3 microstructure, before and after deformation, 100X magnification.

By comparing the raw fusion microstructure of the three specimens, it is evident that the closer the die plate, ie the higher the cooling rate, the more refined the microstructure. As the specimens were laminated, the microstructures behaved similarly, before deformation the grains had the same dimension in all directions, and as they were laminated the grains gradually became elongated along the longitudinal direction. It is noteworthy that the microstructure of the

central region of the sample requires high deformations to reflect changes in its structure, since deformation is a superficial process that affects the outermost layer of the specimen more sharply. This is reflected by Figures 6, 7 and 8 which demonstrate an orientation only for high deformations.

3.5 Hardness

The hardness of the pure aluminum used to make the alloy in the present work is equal to 28 ± 0.84 HV and this value was compared with the hardness of the alloy made in the raw melt state and the hardness after successive rolling passes, showing the effect. The addition of tungsten as a reinforcing element and the sensitivity of the cold working alloy as a hardening mechanism are shown in Figure 9.

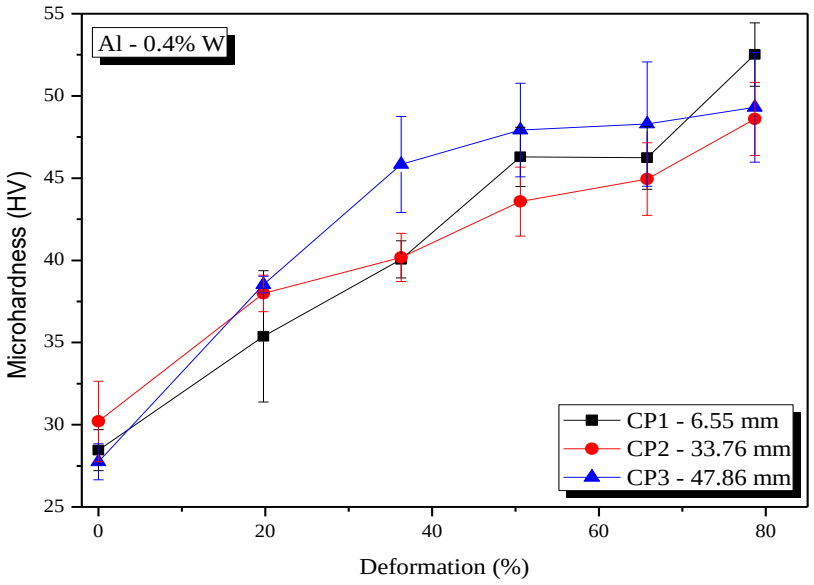

Figure 9. Hardness in the melt and in the rolled state.

Samples taken from different ingot heights showed microhardness values slightly higher than the value found for pure aluminum, leading to believe that tungsten increases the hardness of the aluminum alloy.

According to Reed-Hill (1982), if disagreements are not formed by disagreement generators, then they must be created by a nucleation process that can be homogeneous or heterogeneous. In the case of heterogeneous nucleation means that disagreements are formed with the help of defects present in the crystal, such as solute atom. Thus, justifying the influence of tungsten as a favorable element for the emergence of heterogeneous disagreements in the material that increase its hardness.

It can be inferred that there was macrosegregation effect on the alloy based on the tungsten concentrations indicated in the EDX test which indicated a higher concentration on specimen height two (CP2) and based on the hardness of this sample which was higher than on the other specimens. The fact that the concentration in the farthest specimen of the plate / mold (CP3) does not present higher tungsten concentration may be associated with the effect of the high tungsten density when comparing the aluminum density that may have minimized macrosegregation.

Through the slope of the hardening curves, it is observed that the three specimens respond to the increase of the hardness-increasing strain rates, which corroborates the theory that the disagreement density increases as the material is deformed.

Dieter (1981) states that the stored energy associated with the generation and interaction of disagreements during cold work increases with deformation to a certain extent corresponding to a saturation value. This would justify the fact that CP3 has similar hardness values after the third rolling pass.

It can be observed that of the three specimens analyzed, the specimen with the finest microstructure (CP1) responded best to cold work as mechanisms of lifting hardness, presenting increasing elevation rate and the highest hardness at the end, when compared to other specimens. This is because, in a more refined structure, the amount of grain boundary is greater and this grain boundary makes it difficult to move disagreements.

In quantitative terms, the lamination process promoted a 54% hardness increase in CP1, 62% hardness in CP2 and 56% hardness in CP3 for area reduction of 79%.

Since the hardness of the material has increased, it can be inferred that there was part hardening and consequent increase in tensile strengths (Tiryakioglu et al, 2015).

The lamination process directs the grain direction towards the lamination in such a way that it imposes anisotropy on the material. Such relationship is illustrated in Figures 10, 11 and 12 which demonstrate the difference between the longitudinal hardness to the rolling direction and the hardness transverse to the rolling direction.

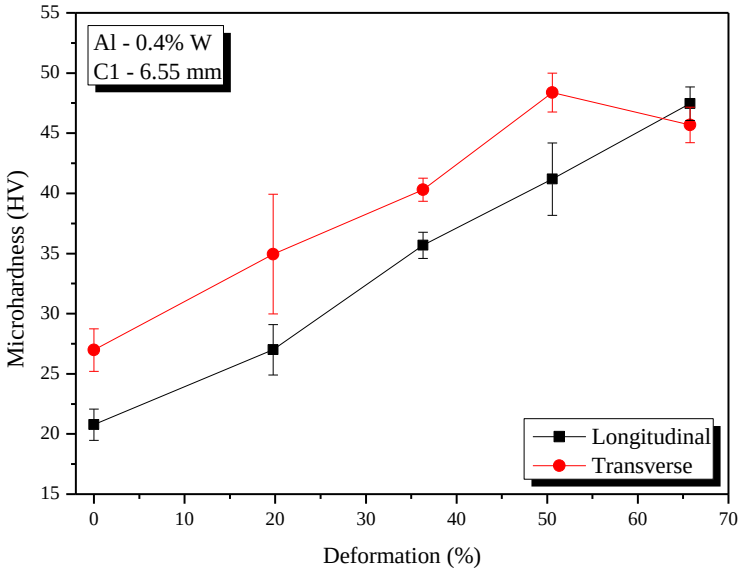

Figure 10. Comparison of longitudinal and transverse microhardness of the specimen at C1 - 6.55 mm.

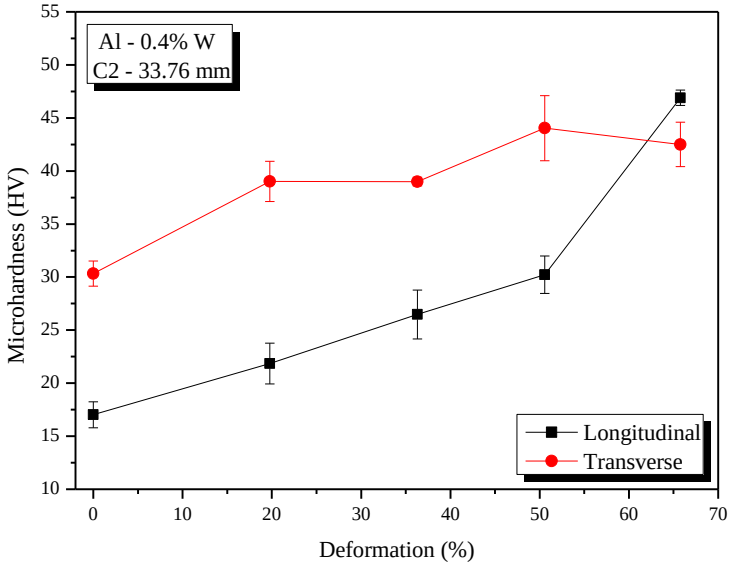

Figure 11. Comparison of longitudinal and transverse microhardness of the specimen at C2 - 33.76 mm.

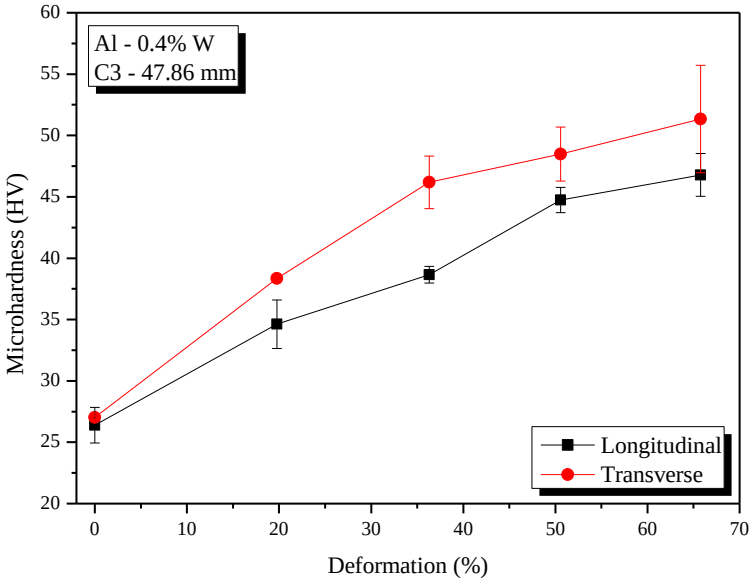

Figure 12. Comparison of longitudinal and transverse microhardness of the specimen at C3 – 47.86 mm.

It is observed that the hardness transverse to the rolling direction is higher than the hardness in the direction parallel to the deformation, which corroborates with the literature since with the elongated grains present larger amounts of grain boundaries in the transverse direction of rolling.

In quantitative terms the differences between longitudinal and transverse hardness were approximately 30% for CP1, 78% for CP2 and 19% for CP3.

By analyzing the hardness variation imposed by the lamination it can be concluded that the specimen two, distant 30.76 mm from the mold plate had the largest increase in percentage hardness and presented the largest percentage difference between its longitudinal and transverse hardness. This was because, since the grains were longer in the longitudinal direction, the anisotropy of the sample was larger. The fact that this sample behaves differently from the behavior of other samples may be associated with the higher presence of tungsten at this point pointed out by the EDX.

4. CONCLUSIONS

As expected, the experimentally obtained values for VL and $\dot{T}$ decrease with the advancement of the liquidus isotherm, thus concluding that the farther from the plate / mold the experimental parameters decrease. They are described by the experimentally obtained laws $V_L = 2.44\ (P_L)^{-0,25}$ e $\dot{T} = 54.91\ (P_L)^{-0,6}$.

Following the literature data for aluminum alloys, it was found that higher cooling rates produced more refined microstructures.

The samples taken from different ingot heights presented microhardness values slightly higher than the value found for pure aluminum, leading to believe that tungsten sensitively increases the hardness of the aluminum alloy, but for this percentage this fraction is so small that has no advantage for the hardness of aluminum in the raw melt state over other alloying elements. However, more studies with increase of solute content are needed to verify the behavior in order to verify if the results show a tendency for this material.

Cold work proved to be an efficient mechanism of hardness increase, promoting 54% hardness increase in CP1, 62% hardness in CP2 and 56% hardness in CP3, for the area reduction of 79%.

The specimen with higher tungsten concentration showed higher sensitivity to cold work showing greater percentage hardness increase, inferring that the addition of tungsten influences the disagreement movement.

An increase in the tensile strengths of the material as it is laminated is inferred due to the increased hardness and the association of these two properties.

5. REFERENCES

ASSOCIAÇÃO BRASILIERA DE NORMAS TÉCNICAS. NBR 13284:Preparação de corpos-de-prova para análise metalográfica – Procedimento, 1995

ASM Handbook Vol. 2, 1992. Properties and Selection: Nonferrous Alloys and Special,– Purpose Materials ASM International (American Society for Metals).

ASM Handbook Voume 9: Metallography and Microstructures. [s.1:s.n].

Calçada, M. V., 2018. *Avaliação mecânica e microestrutural da liga de alumínio AA3104 empregada na indústria de fabricação de latas laminadas à frio com e sem interpasses*. Me.Thesis, Universidade Estadual Paulista. São Paulo, Brazil.

Chiaverini, V., 1986 Tecnologia Mecânica Processos de Fabricação e Tratamento Volume II. 2 ed. São Paulo: McGraw-Hill.

Coutinho et al., 2019. Upward Unsteady-State Solidification of Dilute Al–Nb Alloys: Microstructure Characterization, Microhardness, Dynamic Modulus of Elasticity, Damping, and XRD Analyses. Metals vol .9, n.6, p.713

Coutinho, M. M., 2018. Correlação entre as Propriedades Mecânicas e Microestruturais da Liga Al0,4%Nb em Diferentes Condições de Solidificação. Me. Thesis, Universidade de Brasília, Distrito Federal, Brasil.

Dieter, G.E., 1981*: Metalurgia Mecânica*. 2 ed, Editora Guanabara Dois.

Freitas, E. S., Rosa, D. M., Garcia, A., & Spinelli, J. E., 2011. *Growth of tertiary dendritic arms during the transient directional solidification of hypoeutectic Pb–Sb alloys*. Philosophical Magazine, v. 91, n. 35, p. 4474-4485.

Garcia, A. 2007. *Solidificação: Fundamentos e aplicações*. Editora da Unicamp, São Paulo, 2ºedição.

Helman, H; Cetlin, P. R., 2012. *Fundamentos da conformação- Mecânica dos metais*. Artliber Editora Ltda, São Paulo, 2ª edição.

Oliveira, J. C. P. T., 2009. *Evolução da microestrutura e da textura durante a laminação a frio e a recristalização de alumínio com diferentes níveis de pureza*. Dr. Thesis. Escola Politécnica da Universidade de São Paulo. São Paulo, Brazil.

Pisch, A.; Pasturel, A., 2019. *On the partial enthalpy of mixing of Nb in liquid Al*. *Thermochim*. Acta v. 671, p. 103–109.

Reed-Hill, R. E., 1982. *Princípios de Metalurgia Física*. Guanabara Dois S.A, Rio de Janeiro, 2º edição.

Reyes, R. V. et al., 2017. "*Tensile properties and related microstructural aspects of hypereutectic Al-Si alloys directionally solidified under different melt superheats and transient heat flow conditions".* Materials Science and Engineering: A, v. 685, p. 235–243.

Rodrigues, A. V. et al, 2018. "*Microstructure and Tensile/Corrosion Properties Relationships of Directionally Solidified Al–Cu–Ni Alloys*". Metals and Materials International, v. 24, n. 5, p. 1058–1076.

Rosa, D. M. 2007. *Estruturas Celulares, Transição Celular/Dendrítica e Estruturas Dendríticas na Solidificação Unidirecional Transitória*. Dr. Thesis, Universidade Estadual de Campinas, São Paulo, Brazil.

Şahin, M. et al., 2018. "*Microstructural evolution and mechanical properties of Sn-Bi-Cu ternary eutectic alloy produced by directional solidification*". Materials Research, v. 21, n. 2.

Sousa, T. P., 2019. Evolução da microestrutura bruta de fusão de ligas Al-Cu-Nb solidificadas unidirecionalmente. Me. Thesis. Universidade de Brasília, Distrito Federal, Brazil.

Tiryakioglu et al., 2015 *Hardness-Strength Relationships in the Aluminum Alloy 7010*. Material Science and Engineering A, vol. 631, p.196-200.

6. RESPONSIBILITY NOTICE

The authors are the only responsible for the printed material included in this paper.